TOC

5 A new glucometer-based enzyme immunoassay was developed for sensitive detection of alpha-fetoprotein by using biofunctional dendritic polyaniline nanofiber as the signal-transduction tag.

PAPER

Biofunctionalized dendritic polyaniline nanofiber for *in situ* amplified glucometer-based enzyme immunoassay of tumor marker

Sheng Wu,* Jinsuo Chen, Yujian Tian, Xiaoming Tang, Wei Li and Jieming Li

This work reports on a new electrochemical enzyme immunoassay for sensitive detection of disease-related protein (alpha-fetoprotein, AFP, used as a model target analyte) at a low concentration by using biofunctional dendritic polyaniline nanofiber as the signal-transduction tag. The signal was amplified on basis of glucoamylase-labeling multi-armed dendritic polyaniline nanofiber conjugated with anti-AFP

10 detection antibody. The assay was carried out on an anti-AFP capture antibody-coated microplate with a sandwiched-type immunosensing protocol, and monitored by a portable personal glucometer (PGM). Accompanying formation of the sandwiched immunocomplex in the microplate, the carried glucoamylase by the nanofiber could hydrolyze amylopectin into glucose, and the as-produced glucose could be determinated by the PGM. The detectable signal increased with the increasing target AFP concentration

15 in the sample, and exhibited a wide dynamic range of $0.1 - 50$ ng mL^{-1} with a low detection limit of 0.03 ng mL^{-1} at S/N =3. Meanwhile, the PGM-based enzyme immunoassay displayed high reproducibility and specificity. The assayed results for 15 human serum specimens with PGM-based immunoassay gave a well matched data obtained from the referenced enzyme-linked immunosorbent assay (ELISA) method.

Introduction

20 A simple and sensitive method for monitoring and quantifying the disease-related protein at a low concentration is very important in clinical diagnostics and treatments.[1,2] Immunoassay, based on the specific antigen-antibody recognition for monitoring the antigen or antibody concentration, is usually employed as an alternative

25 scheme for this purpose.[3] More sophisticated analytical devices have been reported and developed for immunoassay development based on different transducers, *e.g.*, surface plasmon resonance, quartz crystal microbalance, fluorescence, chemiluminescence and electrochemical method.[4-9] Unfavorably, most methods

30 involve in expensive instrumentations and professional personnel, and are not suitable routine use, particularly for the developing countries. An alternative immunosensing strategy that utilizes the low-cost, user-friendly and simple instrumentations for assay development would be advantageous.

35 Personal glucometer (PGM) is currently one of the most widely used diagnostic devices in the world because of its portable size, easy operation, low cost, and reliable quantitative results.[10,11] More interestingly, Tang's group recently developed a series of PGM-based detection schemes for quantitative monitoring of

40 aflatoxin B$_1$, brevetoxin B, ATP and lead ion by coupling with target-triggered glucose release from mesoporous nanocontainers.[12-15] Lu,[16] Yang[17] and Xiang[18] groups also utilized the personal glucometer to develop some highly efficient assay modes for non-glucose target analytes by using invertase as the

45 labels. Herein, our motivation is still to employ the personal glucometer as the signal generation device for the development of enzyme immunoassay.

Typically, the PGM signal can be achieved through enzyme-labeled detection antibody. However, the detectable sensitivity is

50 relatively low usually because of the limitation of enzyme-labeled amount on one antibody.[19] We might suspect that if more enzyme molecules could be simultaneously conjugated onto the detection antibody, the sensitivity could be improved. The rapid emergence of bionanotechnology opens a new horizon for the nano labels for

55 signal amplification.[20,21] Recent research has looked to develop innovative and powerful biofunctional nanomaterials, controlling and tailoring their properties in a very predictable manner to meet the needs of specific applications.[22,23] Conducting polymers such as polyaniline have been used as versatile matrices to embed the

60 biomolecules.[24] Compared with bulk and other morphologies of polyaniline, polyaniline nanofiber is subject to secondary growth of irregularly shaped particles, and characteristically disperses in water and other solvents.[25,26] Gao et al. fabricated a polyaniline nanofiber array on poly(etheretherketone) to induce enhanced

65 biocompatibility and controlled behaviors of mesenchymal stem cells.[27] Fang et al. utilized polyaniline nanofiber for immobilization glucose oxidase to extend the lifetime of sensors.[28] Cui et al. developed a sensitive electrochemical immunoassay by means of modifying peroxidase and detection

70 antibody onto dendritic polyaniline nanofiber.[29] Experimental results indicated that the biomolecules including bioactive enzyme and antibody could be conjugated onto the polyaniline nanofiber. Meanwhile, the conjugated biomolecules displayed high bioactivity. To the best of our knowledge, however, there is

75 no report focusing on multi-armed dendritic polyaniline nanofiber

for development of PGM-based enzyme immunoassay.

Alpha-fetoprotein (AFP, a major mammalian embryo-specific and tumor-associated protein) is present in small quantities in adults at normal conditions. The AFP expression is often associated with hepatoma and teratoma and has been widely used as a diagnostic biomarker for hepatocellular carcinoma.[30] In this contribution, we report on the proof-of-concept of a simple and powerful electrochemical immunoassay for sensitive detection of AFP in anti-AFP capture antibody-coated microplate by using the personal glucometer as the detection device. To achieve a high PGM signal, the signal-transduction nanotag is prepared through conjugation of glucoamylase and anti-AFP detection antibody onto the multi-armed polyaniline nanofiber. In the presence of target AFP, a sandwiched immunocomplex can be formed on the microplate between capture antibody and detection antibody. Upon addition of amylopectin, the glucoamylase accompanying the polyaniline nanofiber can hydrolyze it into glucose. The as-produced glucose can be detected by using personal glucometer, thus resulting in the increment of PGM signal with the increasing target AFP concentration in the sample.

Experimental

Materials and reagent

Monoclonal mouse anti-human AFP antibody (mAb$_1$, ascites fluid, clone C3) and polyclonal rabbit anti-human AFP antibody (pAb$_2$) were purchased from Sigma-Aldrich (Shanghai, China). Human AFP ELISA kit was obtained from Amyjet Sci. Inc. (Abcam, China). High-binding polystyrene microplate was achieved from Greiner Bio-one (Frickenhausen, Germany). Glucoamylase (140 000 units mL^{-1}), amylopectin from potato starch, glutaraldehyde and bovine serum albumin (BSA) were purchased from Sigma-Aldrich. Aniline monomer solution (99.5 wt %) was acquired from Sinopharm Chem. Re. Co. Ltd. (Shanghai, China). All other reagents used in this study were of analytical grade. Ultrapure water obtained from a Millipore water purification system (18.2 MΩ cm^{-1}, Milli-Q, Millipore) was used in all runs. Phosphate-buffered saline (PBS, 0.1 , pH 7.4) was prepared by using 0.1 M NaH$_2$PO$_4$ and 0.1 M Na$_2$HPO$_4$, and 0.1 M KCl was used as the supporting electrolyte.

Note: All experiments were carried out in compliance with the relevant laws and institutional guidelines, whilst the institutional committees have approved the experiments.

Synthesis of dendritic polyaniline nanofiber (DPANF)

The dendritic polyaniline nanofiber (designated as DPANF) was prepared referring to the literature.[31] Briefly, 10 mL of the mixture containing 1.5-mL aniline monomer (99.5 wt %) and 8.5-mL HCl (1.0 mol L^{-1}) was initially added quickly into 10 mL of 1.0 mol L^{-1} HCl containing 0.1 mol L^{-1} ammonium persulfate. Afterward, the mixture was reacted for 24 h at room temperature under vigorous shaking on an end-over-end shaker (MS, IKA GmbH, Staufen, Germany). Following that, the black suspension was centrifuged for 20 min at 10 000g, and washed twice with distilled water. Finally, the pellet (*i.e.*, dendritic polyaniline nanofiber) was dispersed into 5-mL distilled water for further usage.

Conjugation of DPANF with glucoamylase and pAb$_2$

The as-synthesized DPANF was conjugated with glucoamylase and pAb$_2$ antibody similar to the literature.[29] Initially, 50-μL glucoamylase (140 000 units mL^{-1}) and 10-μL pAb$_2$ (1.0 mg mL^{-1}) were added to 1-mL of the above-prepared DPANF, and then the mixture was gently shaken for 2 h at room temperature in order to make the biomolecules adsorb to the DPANF. After that, 3 mL of ammonium sulfate (0.35 g mL^{-1}) was injected into the mixture and incubated for another 60 min under the same conditions. During this process, free glucoamylase and pAb$_2$ molecules were precipitated again on the DPANF. Following that, 4 mL of glutaraldehyde (0.5%, v/v) was thrown into the suspension to conjugate the biomolecules for each other. Subsequently, the resulting suspension was centrifuged for 15 min at 10 000g, and the precipitate (*i.e.*, glucoamylase and pAb$_2$-conjugated DPANF, designated as En-DPANF-pAb$_2$) was dispersed into 2-mL PBS, pH 7.4, for the detection of AFP.

PGM-based measurement toward target AFP

Scheme 1 gives the measurement process of PGM-based enzyme immunoassay on mAb$_1$-coated microplate by using En-DPANF-pAb$_2$ as the signal-transduction nanotag with a sandwich-type immunoassay format. Before measurement, monoclonal mouse anti-human AFP antibody-coated microplate was prepared as follows: A high-binding polystyrene 96-well microtiter plate was coated overnight at 4 °C with 50 μL per well of mAb$_1$ (10 μg mL^{-1}) in 0.05 mol L^{-1} sodium carbonate buffer (pH 9.6) (*Note*: To prevent evaporation the microplate was covered with adhesive plastics plate sealing film). Following that, the microplate was washed three times with PBS, and incubated with 300 μL per well of blocking buffer for 60 min at 37 °C with gentle shaking. The microplate was then washed as before. Afterward, 50 μL of AFP standard/sample and 50 μL of the above-prepared En-DPANF-pAb$_2$ were added to the microplate in sequence, and incubated for 40 min at 37 °C under shaking, respectively. The microplate was washed again, and 50 μL of amylopectin (0.5 mg mL^{-1}) in PBS was added to the microplate and hydrolyzed for 50 min at 50 °C. Finally, a 3-μL aliquot of the supernatant was dropped onto the PGM for glucose readout. The PGM signal was registered as the sensing signal relative to different-concentration target AFP. All determinations were made at least in duplicate. The calibration curve was calculated through mathematically fitting experimental points using the Rodbard's four-parameter function with Origin 6.0 software. Graphs were plotted in the form of PGM signal against AFP concentration.

Results and discussion

Design of PGM-based immunoassay with En-DPANF-pAb$_2$

In this work, the PGM signal mainly derived from the hydrolyzed product (glucose) through the conjugated glucoamylase on the polyaniline nanofiber toward the enzyme substrate (amylopectin). Use of multi-armed dendritic polyaniline nanofiber was expected to increase the immobilized amount of glucoamylase molecules, and enhance the sensitivity of PGM-based immunoassay. In order to successfully synthesize polyaniline nanofiber, aniline monomer was initially reacted with HCl to form a new aniline polymer, and then the polymer was further grown with the help of ammonium persulfate. The formed mechanism of polyaniline nanofibers was

described in detail in the literatures.[32,33] The labeling process of glucoamylase and pAb_2 antibody on the polyaniline nanofiber mainly consisted of adsorption, precipitation and cross-linkage. Monoclonal mouse anti-human AFP antibody was coated onto the microplate through the physical interaction between protein and high-binding polystyrene microplate. Upon addition of target AFP, the En-DPANF-pAb_2 was assembled to the microplate through the specific antigen-antibody interaction. Accompanying pAb_2 detection antibody, the carried glucoamylase followed by DPANF could hydrolyze the amylopectin into glucose. By using an external glucometer, the as-produced glucose could be monitored according to the readout. The signal was indirectly proportional to the concentration of target AFP.

Fig. 1A shows typical transmission electron microscope (TEM, Hitachi 7650, Japan) of the as-prepared polyaniline nanofibers. A multi-armed star-like nanostructure could be obviously observed, whilst most polyaniline nanofibers were interweaved with each other through the binding between the end branches. Such a topological structure could provide a large surface coverage for the conjugation of glucoamylase and pAb_2 antibody. When glucoamylase and pAb_2 antibody were conjugated to the dendritic polyaniline nanofiber, the surface became more rougher relative to pure DPANF (Fig. 1B). Logically, we would also ask whether glucoamylase and pAb_2 could really conjugate to the polyaniline nanofibers by our designed route. To clarify this issue, the as-prepared DPANF and En-DPANF-pAb_2 were used for reaction with the amylopectin solution, respectively. The resulting products were determined by using PGM (Fig. 1C). As seen from curve '*a*', the digital signal of amylopectin solution was not almost changed before and after reaction with the DPANF, indicating that the as-synthesized DPANF could not hydrolyze the amylopectin into glucose. When the amylopectin solution incubated with En-DPANF-pAb_2, however, PGM signal increased with the increasing reaction time and then tended to level off (curve '*b*'). The result revealed that the glucoamylase could be conjugated onto the DPANF by the developed method.

Further, we also investigated whether pAb_2 detection antibody was labeled onto the DPANF. By the same token, the as-prepared En-DPANF-pAb_2 was utilized for the detection of zero analyte and 20 ng mL^{-1} AFP on mAb$_1$-coated microplate with a sandwich -type immunoassay protocol, respectively. Following that, the PGM signal was collected and recorded intermittently (every 5 minutes) after addition of amylopectin into the microplate (Fig. 1D). As shown from curve '*a*', the PGM signals were not almost shifted within the reaction times. Significantly, the PGM signal largely increased after 40 min (relative to the initial signal) in the presence of target AFP (curve '*b*'). The increase in the PGM signal was ascribed to the specific antigen-antibody reaction. In the absence of target AFP, the functionalized polyaniline nanofibers could not be assembled to the microplate even if pAb_2 was labeled to the DPANF. In contrast, introduction of target AFP could induce the assembly of functional nanofiber, and cause the change in the PGM signal. On the basis of the comparative study between two methods, we might make a conclusion that pAb_2 was labeled to the DPANF.

Comparative study with and without DPANF

To further elucidate the amplification efficiency of the DPANF toward PGM-based enzyme immunoassay, we prepared two types of the signal-transduction tags, *e.g.*, En-DPANF-pAb_2 and glucoamylase-labeled pAb_2 (En-pAb_2, which was prepared referring to the report[34]), which were used for the detection of 20 ng mL^{-1} AFP on mAb$_1$-coated microplate with the same assay protocol, respectively. The judgment was based on the change in PGM signal relative to the background signal. As seen from Fig.

2, the presence of DPANF could cause a 9.5 ± 1.1 (mM) signal increase of the PGM-based immunoassay, while the signal only increased to 5.2 ± 0.8 mM without the DPANF. The reason might be attributed to the fact that the dendritic polyaniline nanofiber conjugated more glucoamylase molecules than that of En-pAb_2. When one pAb_2 antibody reacted with target AFP, all labeled glucoamylase molecules on DPANF could carry over and take part in the hydrolytic reaction, thus resulting in the amplification of digital signal.

Optimization of experimental conditions

To achieve an optimal digital signal, the conjugation amount of glucoamylase on the DPANF should be studied. In this case, we not only ensured the possibility of the antigen-antibody reaction, but also expected a high digital signal since glucoamylase and pAb_2 were co-immobilized onto the DPANF. As seen from Fig. 3A, the strong PGM signal could be obtained at the volume ratio of 5 : 1 for glucoamylase and pAb_2 (20 ng mL^{-1} AFP used in this case). So, 50-μL glucoamylase (140 000 units mL^{-1}) and 10-μL pAb_2 detection antibody (1.0 mg mL^{-1}) was used for the preparation of En-DPANF-pAb_2 into 1.0 mL of the as-prepared DPANF colloids.

Another important concern on digital signal of PGM-based immunoassay was the hydrolysis time of glucoamylase toward the amylopectin. Usually, it takes some time for the bioactive enzyme to catalyze enzymatic substrate. As seen from Fig. 3B, a relatively strong digital signal could be recorded after 50 min towar 50 ng mL^{-1} AFP (used in this case), indicating that the hydrolysis reaction of glucoamylase tended to the equilibrium. So, 50 min was chosen for enzymatic hydrolysis reaction.

Calibration plots toward target AFP

Under optimal conditions, the sensitivity and working range of the PGM-based enzyme immunoassay was studied by assaying routine samples with different AFP standards on mAb$_1$-coated microplate by using En-DPANF-pAb_2 as the signal-transduction tag. As shown from Fig. 4A, we could clearly observe that with the increasing AFP concentration in the sample the digital signal of the glucometer increased accordingly. A linear dependence between the PGM signal (mM) and AFP concentration (ng mL^{-1}) was achieved in the range from 0.1 to 50 ng mL^{-1}. The linear regression equation was y (mM) = $0.5789 \times C_{[AFP]} - 0.8592$ (ng mL^{-1}, R^2 = 0.9913, n = 21) with a detection limit (LOD) of 0.03 ng mL^{-1} at the $3s_{blank}$ criterion. For comparison, we also investigated the LOD of using En-pAb_2 as the signal-transduction tag (*i.e.*, without DPANF), which was 0.8 ng mL^{-1}. Obviously, the LOD of using DPANF was lower than those of commercialized human AFP ELISA kits (*e.g.*, 2.0 ng mL^{-1} from Abnova CAT# KA0202; 0.15 ng mL^{-1} from Abnova CAT# KA1024; 0.35 ng mL^{-1} from Abcam CAT# ab108680; 0.15 ng mL^{-1} from Abcam CAT# ab108838; 0.31 ng mL^{-1} from Abcam CAT# ab193765). Such a low LOD was possibly ascribed to the *in situ* signal amplification by the massive glucoamylase on the DPANF and the high hydrolytic capacity of glucoamylase toward the enzymatic substrate, amylopectin.

### Reproducibility and specificity

To investigate the precision of PGM-based enzyme immunoassay, the as-prepared En-DPANF-pAb_2 conjugates were utilized for the detection of 5.0 ng mL^{-1} and 20 ng mL^{-1} AFP in mAb$_1$-coating microplates. As shown from Fig. 4B, the relative standard

deviation (RSD, n = 8) values were 6.9% for 5.0 ng mL^{-1} AFP and 4.3% for 20 ng mL^{-1} AFP, respectively, indicating high precision and reproducibility.

To further relegate the differences in response between En-DPANF-pAb$_2$ conjugates to interference degree or crossing recognition level, cancer antigen 125 (CA 125), cancer antigen 15-3 (CA 15-3) and carcinoembryonic antigen (CEA) were added into the microplate, respectively. As indicated from Fig. 5A, a high PGM signal could be only achieved toward target AFP, and other interfering materials did not cause the significant change relative to the control test. The results suggested that the PGM-based enzyme immunoassay had high specificity toward target AFP.

### Analysis of real samples and method comparison

To realize the possible application for the newly developed PGM-based immunoassay in the real samples, we collected 15 human serum specimens containing different-concentration AFP from our hospital (clinical Laboratory and Medical Diagnostics Laboratory) in strict accordance with the Rules of Local Ethical Committee. Before measurement, these specimens were gently shaken at room temperature (*Note*: all handling and processing were performed carefully, and all tools in contact with patient specimens and immunoreagents were disinfected after use), and then monitored by using the PGM-based enzyme immunoassay. Meanwhile, the assayed results were compared with those obtained by the commercialized available Abcam human AFP ELISA kit. As seen from Fig. 5B, the linear regression equation for these data between two methods is as follows: $y = 0.8882x + 4.3228$ (R^2 = 0.9838, n = 45) (x-axis: by PGM-based enzyme immunoassay; y-axis: by AFP ELISA kit). There is no significant difference between the results given by two methods, indicating that the PGM-based immunoassay can provide a promising alternative scheme for determining AFP in human serum during clinical diagnostics.
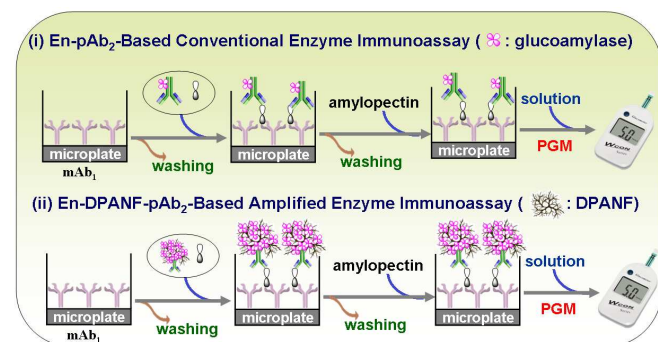

Scheme 1 Schematic illustration of PGM-based enzyme immunoassay in mAb$_1$-coated microplate by using different signal-transduction tag: (i) En-pAb$_2$-based conventional enzyme immunoassay and (ii) En-DPANF-pAb$_2$-based amplified enzyme immunoassay, based on glucoamylase-hydrolyzed amylopectin.
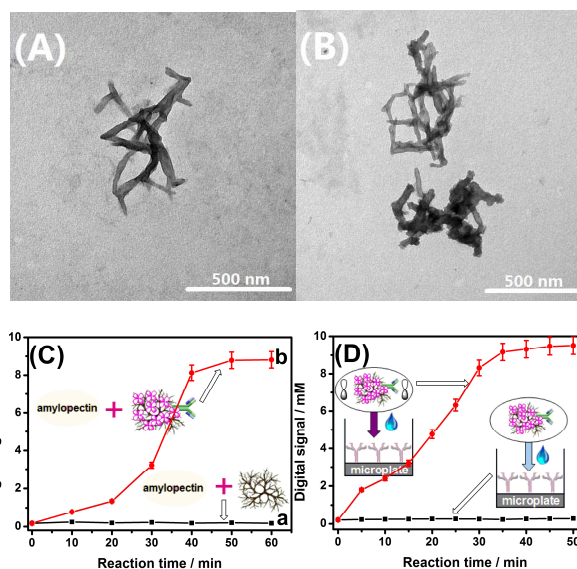

Fig. 1 Typical TEM images of (A) DPANF and (B) En-DPANF-pAb$_2$, (C) digital signal (versus reaction time) of (a) DPANF + amylopectin and (b) En-DPANF-pAb$_2$ + amylopectin, and (D) digital signal (versus reaction time) of (a) mAb$_1$ + En-DPANF-pAb$_2$ and (b) mAb$_1$ + 20 ng mL^{-1} AFP + En-DPANF-pAb$_2$. Error bar represents the standard deviation (n = 3).
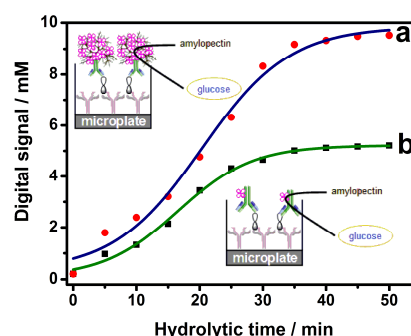

Fig. 2 PGM responses (*vs*. hydrolytic time) of mAb$_1$-coated microplate toward 20 ng mL^{-1} AFP by using different signal-transduction tags: (a) En-DPANF-pAb$_2$ and (b) En-pAb$_2$. Each data represents the average value of three measurements (n = 3).
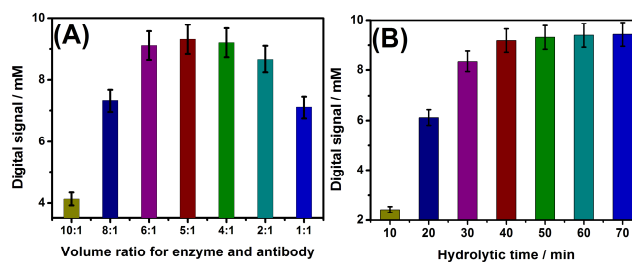
Fig. 3 The effects of (A) volume ratio between glucoamylase (140 000 units mL^{-1}) and pAb$_2$ (1.0 mg mL^{-1}) for the preparation of En-DPANF-pAb$_2$, and (B) hydrolysis time of the labeled glucoamylase on En-DPANF-pAb$_2$ toward amylopectin on the readout signal of PGM-based enzyme immunoassay (20 ng mL^{-1} AFP used in this case) . Error bar represents the standard deviation (n = 3).
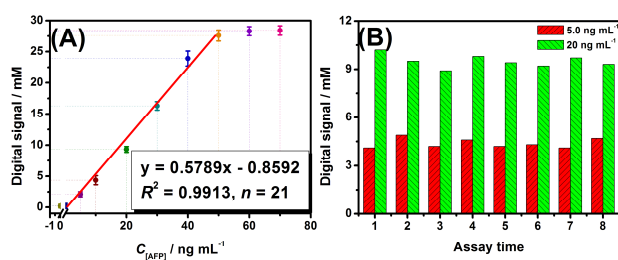
Fig. 4 (A) Digital signals of PGM-based enzyme immunoassay toward AFP standards with different concentrations in mAb_1-coated microplate by using En-DPANF-pAb_2 as the signal-transduction ta, and (B) the precision and reproducibility of PGM-based enzyme immunoassay toward 5.0 and 20 ng mL^{-1} AFP, respectively. Error bar represents the standard deviation (n = 3).
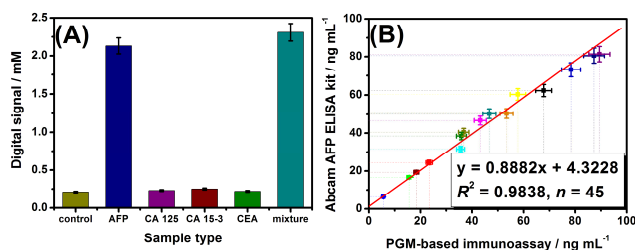
Fig. 5 (A) The specificity of PGM-based enzyme immunoassay against 5 ng mL^{-1} AFP, 50 U mL^{-1} CA 125, 50 U mL^{-1} CA 15-3, and 50 ng mL^{-1} CEA (*Note*: The mixture contained AFP and all interfering materials, and (B) comparison of the assayed results for human serum specimens by using PGM-based enzyme immunoassay and AFP ELISA kit (*Note*: Each data represents the average value of three measurements, whereas the contents of AFP in the specimens were evaluated on the basis of the mentioned-above regression equation: y (mM) = 0.5789 × $C_{[AFP]}$ − 0.8592. High-concentration AFP was calculated according to the dilution ratio). Error bar represents the standard deviation (n = 3).

Conclusions

In the present work, we design a simple and low-cost enzyme immunoassay for sensitive determination of low-abundant protein (AFP used as a model analyte) in biological fluid with glucometer readout in a commercialized microtiter plate by using dendritic polyaniline nanofiber as the nano lable. The detectable signal mainly originated from the labeled glucoamylase on the nanofiber toward the hydrolysis of amylopectin in the detection cell. In comparison with conventional enzyme-labeling strategy alone, introduction of DPANF enhanced the sensitivity of PGM-based immunoassay and improved its analytical performance. Highlight of this work is to simultaneously combine with enzyme label and nano label for *in situ* signal amplification. With the advantages of simplification, low cost, user-friendliness and sensitive readout, the PGM-based enzyme immunoassay has the potential to be utilized by the public, especially developing contries, and opens a new horizon for bioassay development.

Notes and references

40 *Department of Hepatobiliary Surgery, 101th Hospital of Chinese People's Liberation Army, Laparoscopic Surgery Center of Nanjing Military Command, Wuxi, Jiangsu 214044, P.R. China. E-mail: shengwu101@yeah.net or wusheng9999@sina.com; Fax: +86 510 85142101; Tel: +86 510 85142101*

45 1   B. Burton, G. Britton, H. Fang, J. Verhagen, B. Smithers, C. Sabatos-Peyton, L. Carney, J. Gough, S. Strobel and D. Wraith, *Nat. Commun.*, 2014, **5**, 4741.

2   B. Zhang, B. Liu, D. Tang, R. Niessner, G. Chen and D. Knopp, *Anal. Chem.*, 2012, **84**, 5392-5399.

50 3   D. Tang, B. Su, J. Tang, J. Ren and G. Chen, *Anal. Chem.*, 2010, **82**, 1527-1534.

4   S. Wu, Z. Zhong, D. Wang, M. Li, Y. Qi, N. Dai and Z. Li, *Microchim. Acta*, 2009, **166**, 269-275.

5   Y. Adiguzel and H. Kulah, *Biosens. Bioelectron.*, 2015, **65**, 121-138.

55 6   T. He, Y. Wang, P. Li, Q. Zhang, J. Lei, Z. Zhang, X. Ding, H. Zhou and W. Zhang, *Anal. Chem.*, 2014, **86**, 8873-8800.

7   K. Suherman and T. Kawaguchi, *Biosens. Bioelectron.,* 2015, doi:10.1016/j.bios.2014.08.055.

8   M. Li, X. Liu, X. Hua, W. Yin, Q. Fang and M. Wang, *Anal. Method*, 60   2014, **6**, 6541-6547.

9   B. Su, J. Tang, H. Chen, J. Huang, G. Chen and D. Tang, *Anal. Method*, 2010, **2**, 1702-1709.

10   J. Chen, W. Wu and L. Zeng, *Anal. Method*, 2014, **6**, 4840-4844.

11   X. Fu, X. Feng, K. Xu and R. Huang, *Anal. Method*, 2014, **6**, 2233-65   2238.

12   L. Hou, C. Zhu, X. Wu, G. Che and D. Tang, *Chem. Commun.*, 2014, **50**, 1441-1443.

13   D. Tang, Y. Lin, Q. Zhou, Y. Lin, P. Li, R. Niessner and D. Knopp, *Anal. Chem.,* 2014, doi:10.1021/ac503616d.

70 14   Z. Gao, D. Tang, M. Xu, G. Chen and H. Yang, *Chem. Commun.,* 2014, **50**, 6256-6258.

15   L. Fu, J. Zhuang, W. Lai, X. Que, M. Lu and D. Tang, *J. Mater. Chem. B*, 203, **1**, 6123-6128.

16   Y. Xiang and Y. Lu, *Chem. Commun.*, 2013, **49**, 585-587

75 17   L. Yan, Z. Zhu, Y. Zou, Y. Huang, D. Liu, S. Jia, D. Xu, M. Wu, Y. Zhou, S. Zhou and C. Yang, *J. Am. Chem. Soc.*, 2013, **135**, 3748-3751.

18   J. Xu, B. Jiang, J. Xie, Y. Xiang, R. Yuan and Y. Chai, *Chem. Commun.*, 2012, **48**, 10733-10735.

19   D. Tang, Z. Zhong, R. Niessner and D. Knopp, *Analyst*, 2009, **134**, 80   1554-1560.

20   F. Pu, J. Ren and X. Ou, *Adv. Mater.*, 2014, **26**, 5742-5757.

21   C. Lok, T. Zou, J. Zhang, I. Lin and C. Che, *Adv. Mater.*, 2014, **26**, 5550-5557.

22   F. Zhang, J. Nangreave, Y. Liu and H. Yan, *J. Am. Chem. Soc.*, 2014, 85   **136**, 11198-11211.

23   S. Kleijn, S. Lai, M. Koper and P. Unwin, *Angew. Chem. Int. Ed.*, 2014, **53**, 3558-3586.

24   M. Sk, C. Yue and R. Jena, *RSC Adv.*, 2014, **4**, 5188-5197.

25   M. Kotal, A. Thakur and A. Bhowmick, *ACS Appl. Mater. Interface*, 90   2013, **5**, 8374-8386.

26   L. Shao, J. Jeon and J. Lutkenhaus, *J. Mater. Chem. A*, 2013, **1**, 7648-7656.

27   H. Gao, J. Zhang, F. Liu, Z. Ao, S. Liu, S. Zhu, D. Han and B. Yang, *J. Mater. Chem. B*, 2014, **2**, 7192-7200.

95 28   L. Fang, B. Liang, G. Yang, Y. Hu, Q. Zhu and X. Ye, *Biosens. Bioelectron.*, 2014, **56**, 91-96.

29   Y. Cui, D. Tang, B. Liu, H. Chen, B. Zhang and G. Chen, *Analyst*, 2012, **137**, 1656-1662.

30   Z. Wang, X. Chen and Z. Ma, *Biosens. Bioelectron.*, 2014, **61**, 562-100   568.

31   H. Kim, I. Lee, Y. Kwon, B. Kim, S. Ha, J. Lee and J. Kim, *Biosens. Bioelectron.*, 2011, **26**, 3908-3913.

32   H. Kim, I. Lee, Y. Kwon, B. Kim, S. Ha, J. Lee and J. Kim, *Biosens. Bioelectron.*, 2011, **26**, 3908-3913.

105 33   A. Wolfter, P. Rannou, J. Travers, B. Gilles and D. Djurado, *Phys. Rev.*, 1998, **58**, 7636.

34 G. Hermanson, *Bioconjugate Techniques,* 2nd ed.; Academic Press, San
    Diego, 2008; p. 925.